



International Conference on Computational Science, ICCS 2010

# Human mobility and population heterogeneity in the spread of an epidemic

S. Merler<sup>a,\*</sup>, M. Ajelli<sup>a</sup>,

<sup>a</sup>*Bruno Kessler Foundation, Trento, via Sommarive 18, Italy*

---

## Abstract

Little is known on how different levels of population heterogeneity and different patterns of human mobility would affect the course of an epidemic in terms of timing and impact. By employing a large-scale spatially-explicit individual-based model, based on a highly detailed model of the European populations and on a carefully analysis of air and railway transportation data, we provide quantitative measures of their effects at European level. Our results show that Europe must prepare to face a fast diffusion of an epidemic, mostly because of the early importation of the first cases from abroad and the synchronization of the local epidemics, determined by the high mobility of the European population. We found that the cumulative attack rate is positively correlated with the average households size and the fraction of students in the population, and negatively correlated with the fraction of inactive population. These results have potentially strong implications in terms of mitigation and control, and suggest that the effectiveness of interventions as antiviral treatment and prophylaxis, schools closure and travel restrictions should be evaluated on a country basis.

© 2010 Published by Elsevier Ltd.

*Keywords:* Agent-based models, transportation networks, epidemics

---

## 1. Introduction

The spread of an infectious disease epidemic is driven by the interplay of two factors: the transmissibility of the pathogen responsible for the infection and the characteristics of the host population. When the role of host is played by a human population, predicting the spread of an epidemic is a tough problem due the complexity of modern human societies. It is well established that the spatial structure of the population has an impact on the diffusion of an epidemic: measles waves in England and Wales, spreading from large cities to small towns, are determined by the spatial hierarchy of the host population structure [1], and the spatial distribution of farms influences the regional variability of foot-and-mouth outbreaks in United Kingdom [2]. The heterogeneity of the population itself can play an important role in the spread of an epidemic [3]. It is also well known that human mobility patterns affect the spatiotemporal dynamics of an epidemic: the role played by the airline transportation network has been analyzed in [4], and it has been shown that the high degree of predictability of the worldwide spread of infectious diseases is caused by the strong heterogeneity of the transport network [5].

---

\*Corresponding author

Email addresses: [merler@fbk.eu](mailto:merler@fbk.eu) (S. Merler), [ajelli@fbk.eu](mailto:ajelli@fbk.eu) (M. Ajelli)

Large-scale individual-based spatially explicit transmission models of infectious diseases [6] have become a relevant tool to evaluate intervention options for containing [7, 8] or mitigating [9, 10, 11, 12, 13, 14, 15] a new influenza pandemic. A review is given in [16]. Because of their complexity, these models have been developed only at country level, including also some European countries [10, 12].

However, Europe has never been analyzed as a whole and thus it is still uncertain how a new pandemic influenza could spread in Europe. Europe comprises countries characterized by completely different social and economical backgrounds that result in different levels of population heterogeneity, in terms of both sociodemographic structure and mobility. In particular, it is still unclear how differences in the sociodemographic structure, which result in different levels of population heterogeneity, and different patterns of human mobility can affect the spatiotemporal spread of an epidemic. Here we provide quantitative measures of their effects on the impact and the timing of a highly transmissible influenza pandemic at European level.

## 2. Results

### 2.1. Population heterogeneity

By analyzing data on the sociodemographic structure of 37 European countries (see Fig. 1a) provided by the Statistical Office of the European Communities (Eurostat) and integrated with data provided by the National Statistical Offices for countries not covered by Eurostat, we found that the frequencies of household type and size (Fig. 1b-c), the age structure (Fig. 1e), the schools size (Fig. 1d), the rates of school attendance and employment by age (Fig. 1f) are highly variable across Europe. The age structure of countries like Ireland, which is one of the youngest European countries (with 31% of the population aged less or equal than 20 years), differs drastically from that of countries like Germany and Italy (where only 22% and 20.5% of the population is aged less or equal than 20 years, respectively), which are characterized by very low fertility rates [17]. This results in largely different frequencies of household type and size. The fraction of households with children ranges from 0.3 in Denmark to 0.6 in Sweden and the average household size ranges from 2.1 in Denmark to 3 in Cyprus. By restricting our attention to the households with children, a large variability in the number of children per household is also observable, with countries as Ireland and Cyprus, where households have several children, opposite to countries like Germany and Bulgaria. We have also observed a large difference in terms of employment rates in the population aged more than 15 years (the legal working age in Europe is 15 or 16, with some exceptions): the fraction of workers ranges from 0.39 in Bulgaria to 0.67 in Lichtenstein. The fraction of students in the population aged more than 15 years ranges from 0.04 in Denmark to 0.12 in Cyprus. According to the PIRLS 2001 and PISA 2000 and 2003 international surveys, as elaborated in [18], the average size of primary schools ranges from 200 to 750 and the average size of secondary schools ranges from 270 to 1000. We used an independent data set providing information on all the Italian schools to validate the surveys data. Data concerning workplaces in Italy and United Kingdom do not highlight significant differences in the size of workplaces. We used the above described sociodemographic data to generate a highly detailed synthetic population of individuals, explicitly grouped in households, schools and workplaces, for simulating the populations in the different countries of the study area. Since it is reasonable to assume that the epidemiological characteristics of the virus do not vary among the European countries, we should expect that the high variability in the sociodemographic structure of the European countries results in a high variability in the impact of an influenza pandemic in the different European countries. This is the first key issue we want to address. Details on the analysis of the European sociodemographic structure are given in [19].

### 2.2. Human mobility

We analyzed air and railway transportation data as provided by Eurostat. We found that in the 2007 more than 360 millions passengers have taken international trips across EU27 (see Fig. 1a), 323 millions of whom by airplane and 37 millions by train. In the same year, more than 135 millions passengers have entered EU27 from countries outside EU27. The great majority of these travels are from and to the western part of Europe (see Fig. 2a-b), namely United Kingdom, Germany, France, Italy and Spain (about the 85% of the travels are from and to these countries). The probability density function of travel distances is shown in Fig. 2c. As shown in [21, 22], international travel flows are related to economic factors. By considering only the travels across EU27, we found that the flow from country  $i$  to country  $j$  can be explained by a gravity model depending on the GDP (Gross Domestic Product: it is an

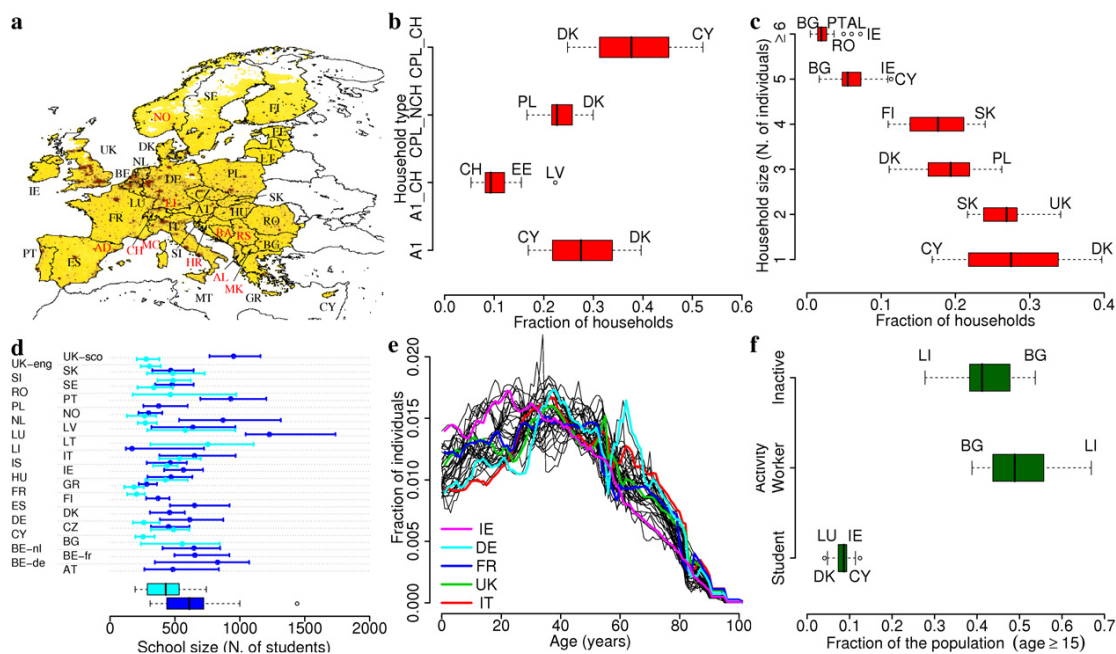


Figure 1: Sociodemographic structures. (a) The study area includes 37 countries and accounts for about 515 millions individuals. Colors from yellow to brown indicate increasing density of population. Black labels refer to countries belonging to EU27 while red labels refer to countries which do not belong to EU27. (b) Variability in the frequencies of household type at European level. A1 represents single persons, A1.CH single parents with children, CPL.NCH couples without children, CPL.CH couples with children. More than 95% of European households are structured as one of the four above mentioned types. (c) Variability in the frequencies of household size. (d) Variability in schools size (primary schools in cyan, secondary schools in blue). Horizontal lines identify the percentiles 25 and 75, the points represent the median values. The two boxplots represent the distributions of the average school size in the different countries. (e) Age structure curves in the different countries. (f) Variability in the employment and school attendance rates. Only individuals aged more than 15 are considered. In the model, individuals aged less or equal than 15 are assumed to attend schools.

economic index measuring the national income and output for a country) per capita, the population and the distance:

$F_{ij} = \theta \frac{g_i^{\tau_f} g_j^{\tau_r}}{d_{ij}^\rho}$ , where  $g_i$  is a normalized GDP of country  $i$  ( $g_i = \frac{G_i}{G^*} p_i$  where  $G_i$  is the GDP per capita of country  $i$ ,  $G^*$  is the average GDP per capita of EU27 and  $p_i$  is the population of country  $i$ ) and  $d_{ij}$  is the distance between the two countries.  $\tau_f$  and  $\tau_r$  tune the dependence of dispersal on donor and recipient sizes and  $\rho$  tunes the dependence on the distance,  $\theta$  is a proportionality constant. To show this, we generated a synthetic population of travelers taking travels according to a gravity model whose masses are given by the normalized GDPs (model A), by the population sizes, as in [23] (model B) and, finally, taking travels by choosing a random destination (model C). We found that model A explains the origin-destination matrix (Fig. 2d) and the distance distribution (Fig. 2e) better than models B and C. This considered, we used model A for simulating long-distance travels across the study area. As for the internal commuting, i.e. daily trips to school and workplace, we adopted the following procedure. First, schools and workplaces of the proper size were spatially-distributed proportionally to the population. Afterward, students and workers were randomly assigned to a school or workplace, in such a way that the resulting distance to school/work distribution complies with a truncated power-law distribution (see Fig. 2f), as proposed in [20] for the radius of gyration of mobile phone users, extending the precursor work presented in [24] on the circulation of bank notes in the United States of America. Commuting flows are found, on average, to be one order of magnitude larger than airline flows [25]. To what extent the observed mobility patterns and their inhomogeneity across the European countries affect the spread of a new influenza pandemic in Europe is the second key issue we want to address. Details on the analysis of human mobility patterns are given in [19].

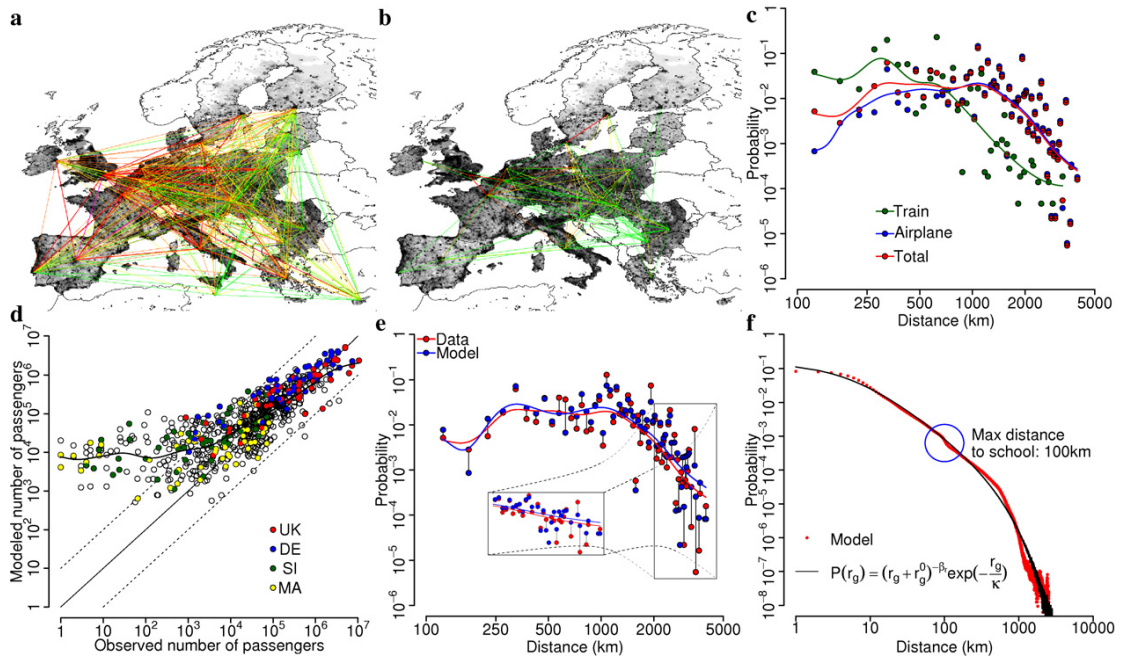


Figure 2: Population movement patterns. (a) Network of yearly airplane travelers across Europe (colors are defined as follows. Green: less than 10,000 travelers, yellow: 10,000 to 100,000 travelers, orange: 100,000 to 1,000,000 travelers, red: 1,000,000 to 10,000,000 travelers, purple: more than 10,000,000 travelers). Each link between two countries is identified by an arc connecting the two capitals. (b) as (a) but for train travelers. (c) Probability density function of travel distances by train (green points), by airplane (blue points) and total (red points). Solid lines represent smooth interpolations of data. (d) Model A) (described in the main text; parameters:  $\tau_f = 0.57$ ,  $\tau_r = 0.99$  and  $\rho = 0.39$ ): comparison between the observed and the modeled origin-destination matrix. Points compare generic entries of the two matrix and the solid black line represents a smooth interpolation. The model tends to overestimate the number of travelers when the actual yearly number of travelers is less than 1,000; it is in good agreement with the data on the most important links. (e) Model A): resulting probability density function of travel distances compared with that resulting from the analysis of the observed data (shown in c) (red points). (f) Internal commuting: probability density function of travel distances to school/workplace (in the model, red points), compared with that proposed in [20] for the radius of gyration of mobile phone users (black points). In the model, students are assumed to attend schools no more than 100km from home. This results in a change in the slope of the probability curve (blue circle).

### 2.3. Spatiotemporal spread of a pandemic influenza in Europe

The transmission rates, defined as the product of the contacts rate times the probability of transmitting the infection, of a new influenza pandemic are unknown. By looking at past pandemics, we can only make assumptions on its transmissibility potential, which can be summarized by the reproductive number  $R_0$  (essentially, the number of secondary infections that result from a single infectious individual in a fully susceptible population [26]). The investigated value is  $R_0 = 2$ . Moreover, according to [10], the model is parametrized so that in the United Kingdom 30% of transmission occurs in households, 37% in schools and workplaces and 33% in the general community. Since the contact rates and, consequently, the reproductive number are determined by the sociodemographic structure of the population we are somehow setting the probability of transmitting the infection in the different social contexts. After having parametrized the model in the United Kingdom, the same transmission rates are assumed in the rest of the study area. In what follows, when not differently stated, we are assuming  $R_0 = 2$  (as discussed, it means  $R_0 = 2$  in the United Kingdom). We assume that the latent period is 1.5days and the infectious period is 2days (however we performed a sensitivity analysis for values of this epidemiological parameter in the range 1.5 - 3days). Infected individuals are assumed to have a probability 0.5 of developing clinical symptoms.

We found that the probability of importing the first case is higher in the western countries (the first case is imported in United Kingdom or Germany in almost 50% of simulations, see Fig. 3a). The distributions of the timing of the

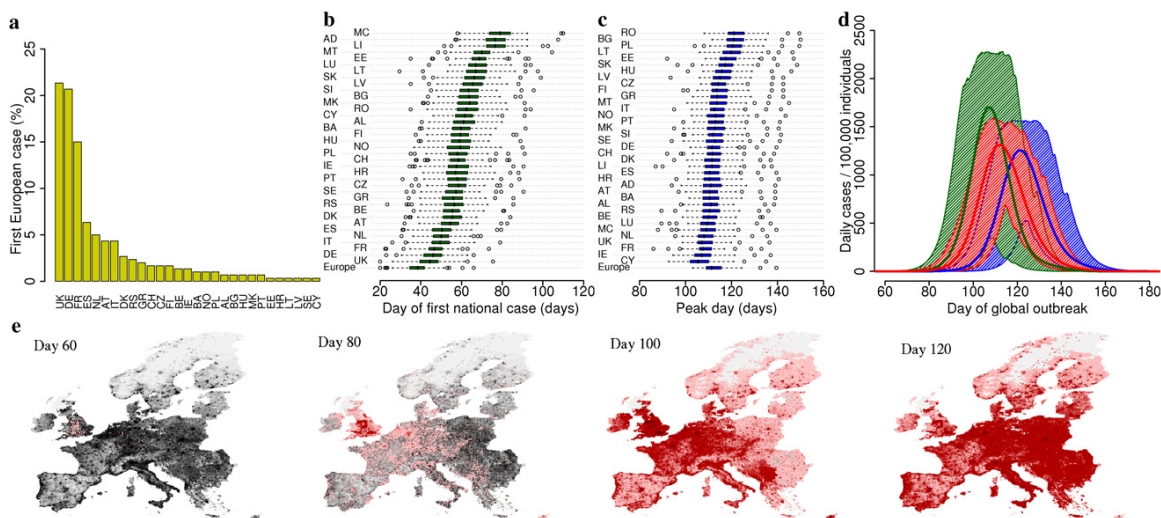


Figure 3: Spatiotemporal dynamics of a new pandemic influenza ( $R_0 = 2$ ). (a) Probable destination of the first case imported in Europe. (b) Distributions of the day of the first national case (days since the first world case) in the different countries. (c) Distributions of the peak day (days since the first world case) in the different countries. (d) Expected number of daily cases per 100,000 individuals in time in Europe (red line) and 95% confidence intervals (shaded area). Green and blue lines (and shaded areas) refer to the expected number of daily cases per 100,000 individuals in Ireland and Bulgaria respectively. These two countries are among those where the impact of the epidemic is expected to be the highest and the lowest respectively. (e) Time sequence (in days) of a simulated epidemic. A single simulation with first European case in United Kingdom is shown. Colors from pink to dark red indicate an increasing number of daily cases (dark red indicates more than 10,000 daily cases).

first case differ largely from country to country (see Fig. 3b): in average, the first case occurs 44 and 79 days after the first world case in the United Kingdom and Principality of Monaco respectively. By ignoring the less populous countries, a west-east gradient is clearly observable. The variability in the peak day in the different countries (see Fig. 3c) is less remarkable (in average it ranges from 106 days in Cyprus to 122 in Romania) since long-distance travels tend to synchronize the national epidemics and these are much faster in the less populous countries. In general, we have observed that the high mobility inside the countries (internal commuting) and the long-distance travels tend to synchronize, thus fastening, the epidemic. The average peak day in a country is positively correlated with the longitude of the country (Spearman test,  $\rho = 0.55$ ,  $p = 0.0003$ ), as confirmed by the clear spatial trend observable in the time sequence of the simulated epidemic shown in Fig. 3e. This finding is supported by the results presented in [27], where a spatial analysis revealed a significant west-east pattern in the timing of peak influenza activity across Europe for the eight winters since 1999–2000. The average peak day in a country is negatively correlated with the yearly number of passengers entering the country from other countries in the study area (Spearman test,  $\rho = -0.59$ ,  $p = 0.001$ ), supporting the hypothesis that the observed pattern of epidemic spread is related to patterns of human movement. The expected pattern of spread in Europe is shown in Fig. 3d. The epidemic peaks some 110 days after the first world case and the epidemic lasts about 3 months. We remark that Fig. 3d reports the expected number of new cases in time. Since the epidemics are not synchronized in time, the actual peak incidence will be much higher than the value corresponding to the peak day reported in the figure (it will be closer to the upper 95% confidence limit, see also Fig. 4b).

In average, the cumulative attack rate in the different countries ranges from 31.2% in Bulgaria to 37.8% in Cyprus (see Fig. 4a). By looking at the study area as a whole, the average cumulative attack rate is 33.7%. Among the most populous countries, the cumulative attack rate is expected to be 31.7% in Germany, 33.4% in the United Kingdom, 33.5% in Italy, 34.5% in France and 35.5% in Spain. It is worth noticing that the value obtained for the United Kingdom is very similar to that obtained in [10]. The standard deviations of the distributions of the national cumulative attack rates are very small, but for the less populous countries. The average cumulative attack rate in a country is

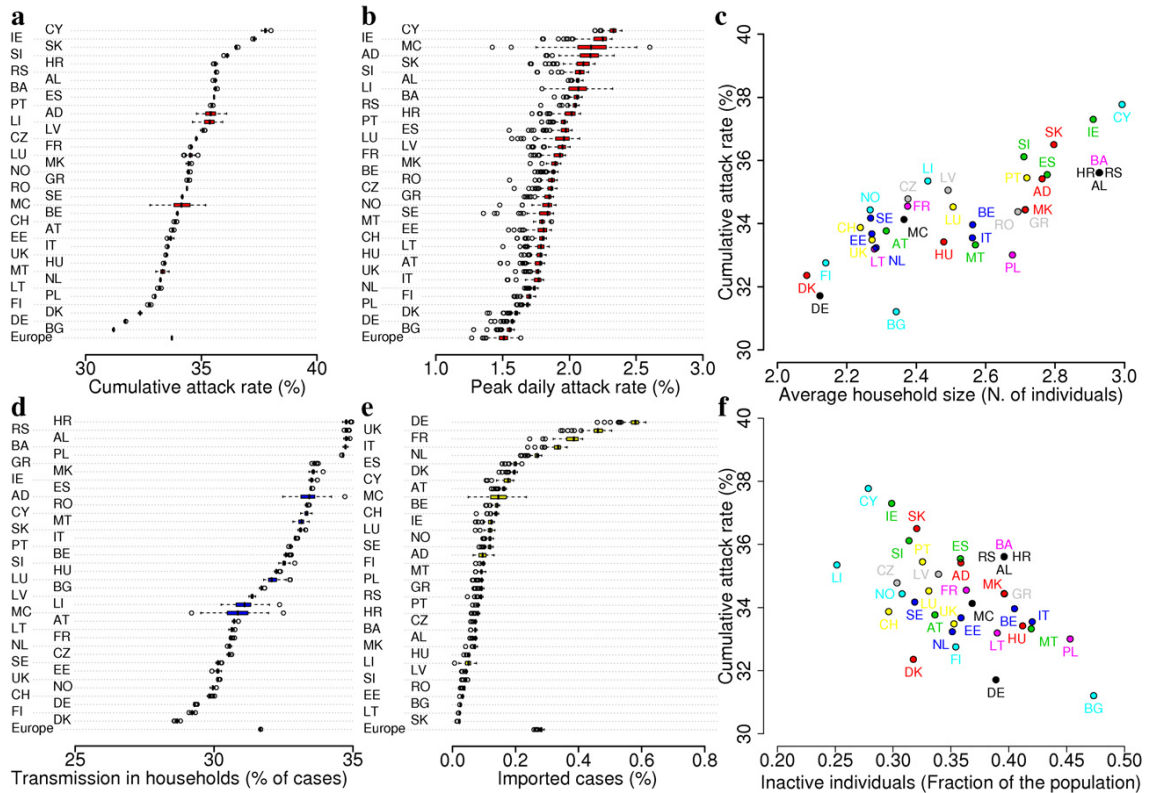


Figure 4: Impact of a new pandemic influenza ( $R_0 = 2$ ). (a) Distributions of the cumulative attack rate in the different countries. (b) Distributions of the peak daily attack rate in the different countries. (c) Average cumulative attack rate as a function of the average household size in the different countries. (d) Distributions of the percentage of cases due to transmission among household members in the different countries. (e) Distributions of the percentage of the population infected during long-distance travels across or outside Europe. (f) Average cumulative attack rate as a function of the fraction of inactive (neither students nor workers) individuals in the different countries.

positively correlated with the average household size (Spearman test,  $\rho = 0.77$ ,  $p < 0.0001$ ) (see Fig.4c) and with the fraction of students in the population (Spearman test,  $\rho = 0.77$ ,  $p < 0.0001$ ), and negatively correlated with the fraction of inactive individuals in the population (Spearman test,  $\rho = -0.38$ ,  $p = 0.02$ ) (see Fig. 4f). It is worth noticing that a simple linear regression model whose independent variables are the average household size, the fraction of students and the fraction of inactive individuals in the population predicts very well the average cumulative attack rate in the different countries (coefficient of determination  $R^2 = 0.985$ , root mean square error RMSE=0.17). The peak daily attack rate in the different countries is also highly variable. It ranges from 1.5% in Bulgaria to 2.3% in Cyprus (see Fig. 4b). Since the national epidemics are not synchronized, the average peak daily attack rate of the whole study is similar to the value observed in Bulgaria, namely 1.5%. In the United Kingdom we obtained a lower peak daily attack rate (1.8%) with respect to the 2.1% as reported in [10]. This is due to different modeling choices for the infective period. We assume an exponential distribution for both latent and infectious period (as in classical mathematical models of infectious diseases) and infectiousness is assumed to be constant during the infectious period (2 days). In [10] individuals transmit more at the very beginning of the infectious period, giving rise to faster simulated epidemics and to higher peak daily attack rates. These different modeling choices can affect the evaluation of some containment strategies (e.g. antiviral treatment) and can lead to differences in the timing of the simulated epidemics but do not affect the results presented in this work. The cumulative attack rate does not depend on the infectious period. Values of peak day and peak daily attack rate in the United Kingdom similar to that reported in [10] were obtained by

assuming an infectious period of 1.5 days. We found that the peak daily attack rate in a country is positively correlated with the average household size (Spearman test,  $\rho = 0.72$ ,  $p < 0.0001$ ) and with the fraction of students in the total population (Spearman test,  $\rho = 0.79$ ,  $p < 0.0001$ ), and slightly negatively correlated with the fraction of inactive individuals in the total population (Spearman test,  $\rho = -0.31$ ,  $p = 0.06$ ). Moreover, it is negatively correlated with the number of inhabitants (Spearman test,  $\rho = -0.51$ ,  $p = 0.001$ ) since the national epidemics tend to be less spatially synchronized in the larger countries. It is also relevant to analyze where transmission occurs. We found that the transmission in households in the different countries ranges from 28.6% in Denmark to 34.8% in Croatia (see Fig. 4d) and that the fraction of the population contracting the infection in foreign countries ranges from 0.02% in Slovakia to 0.57% in Germany (see Fig. 4e). These last results suggest that the efficacy of some targeted interventions, e.g. post-exposure prophylactic antiviral treatment [10, 12] and travel restrictions [28], could be largely different from country to country.

### 3. Methods

We developed an individual-based epidemic simulation model that accounts, at country level, for explicit transmission in households, schools, workplaces (where homogeneous mixing is assumed) and in the general population (where the force of infection is assumed to depend explicitly on the distance). The epidemic can spread from one country to another through cross-border diffusion and because of long distance travels. The infection is continuously sustained in the study area by importation of cases from countries outside Europe. Sociodemographic data were used to generate a highly detailed synthetic population of individuals, explicitly grouped in households, schools and workplaces, for simulating the populations in the different countries of the study area. Data on air and railway transportation data were used to simulate long-distance travels across the countries of the study area and to simulate importation of cases. Details are given in [19].

### 4. Conclusions

Reliable data on the proportion of transmission in social contexts, crucial to the disease transmission, as prisons, leisure places, public transportation systems, hospitals are not available, though some research works are contributing to fill the gap [29, 30]. Spontaneous behavioral changes in the population, as a protective response to a (possibly lethal) epidemic, could affect the spread of the epidemic [31], as well as the imminent school closure in the Summer period. Despite these limitations, our results clearly show that, once the infection will be well established in Europe, European countries have to be prepared to face a fast spread of the epidemic because of the high mobility of the population, resulting in an early importation of the first cases from abroad and in a high synchronization of the local epidemics. Moreover, the number of imported and secondary cases in the initial phase of the epidemic is much larger in the Western side of Europe. The impact of the epidemic is different among the European countries. Specifically, countries as Ireland would have to face more severe epidemic than countries as Germany and Bulgaria because of their sociodemographic structure, characterized by large household groups and by a large fraction of students in the population. Our results are supported by the findings presented in [29], where the authors analyzed social contacts and mixing patterns in eight European countries. Specifically, they found that living in a larger household size was associated with higher number of reported contacts. Moreover, they found that the dominant feature of the contact matrix data is the strong diagonal element: individuals in all age groups tend to mix assortatively (i.e., preferentially with others of similar age) and this pattern is most pronounced in those aged 5–24 years, i.e. the scholar age. They also found that 58% of all reported contacts occur at home, at work, or at school. This result supports our assumption on the proportion of transmission in the different social contexts (in the model, 67% of transmission occurs in households, schools and workplaces, at least in the United Kingdom). These results should have to be taken into account for planning strategies for mitigating future pandemics.

### Acknowledgments

We thank the European Union FP7 FLUMODCONT and EPIWORK projects for research funding.

## References

- [1] B. T. Grenfell, O. N. Bjornstad, J. Kappey, Travelling waves and spatial hierarchies in measles epidemics, *Nature* 414 (6865) (2001) 716–723.
- [2] M. Keeling, M. E. J. Woolhouse, D. J. Shaw, L. Matthews, M. Chase-Topping, D. T. Haydon, S. J. Cornell, J. Kappey, J. Wilesmith, B. T. Grenfell, Dynamics of the 2001 uk foot and mouth epidemic: stochastic dispersal in a heterogeneous landscape, *Science* 294 (2001) 813–817.
- [3] J. Dushoff, S. Levin, The effects of population heterogeneity on disease invasion, *Math Biosci* 128 (1-2) (1995) 25–40.
- [4] V. Colizza, A. Barrat, M. Barthélemy, A. Vespignani, The role of the airline transportation network in the prediction and predictability of global epidemics, *Proc Natl Acad Sci USA* 103 (7) (2006) 2015–2020.
- [5] L. Hufnagel, D. Brockmann, T. Geisel, Forecast and control of epidemics in a globalized world, *Proc Natl Acad Sci USA* 101 (2004) 15124–15129.
- [6] S. Riley, Large-Scale Spatial-Transmission Models of Infectious Disease, *Science* 316 (5829) (2007) 1298–1301.
- [7] I. M. J. Longini, A. Nizam, S. Xu, K. Ungchusak, W. Hanshaoworakul, D. A. Cummings, M. E. Halloran, Containing pandemic influenza at the source, *Science* 309 (5737) (2005) 1083–1087.
- [8] N. M. Ferguson, D. A. Cummings, S. Cauchemez, C. Fraser, S. Riley, A. Meeyai, S. Iamsrithaworn, D. S. Burke, Strategies for containing an emerging influenza pandemic in Southeast Asia, *Nature* 437 (7056) (2005) 209–214.
- [9] I. M. J. Longini, M. E. Halloran, A. Nizam, Y. Yang, Containing Pandemic Influenza with Antiviral Agents, *Am J Epidemiol* 159 (7) (2004) 623–633.
- [10] N. M. Ferguson, D. A. Cummings, C. Fraser, J. C. Cajka, P. C. Cooley, Strategies for mitigating an influenza pandemic, *Nature* 442 (7101) (2006) 448–452.
- [11] T. C. Germann, K. Kadau, I. M. J. Longini, C. A. Macken, Mitigation strategies for pandemic influenza in the United States, *Proc Natl Acad Sci USA* 103 (15) (2006) 5935–5940.
- [12] M. L. Ciofi degli Atti, S. Merler, C. Rizzo, M. Ajelli, M. Massari, P. Manfredi, C. Furlanello, G. Scalia Tomba, M. Iannelli, Mitigation measures for pandemic influenza in Italy: an individual based model considering different scenarios, *PLoS ONE* 3 (3) (2008) e1790.
- [13] M. E. Halloran, N. M. Ferguson, S. Eubank, I. M. Longini Jr, D. A. T. Cummings, B. Lewis, S. Xu, C. Fraser, A. Vullikanti, T. C. Germann, D. Wagener, R. Beckman, K. Kadau, C. Barrett, C. A. Macken, D. S. Burke, P. Cooley, Modeling targeted layered containment of an influenza pandemic in the United States, *Proc Natl Acad Sci USA* 105 (12) (2008) 4639.
- [14] S. Merler, M. Ajelli, C. Rizzo, Age-prioritized use of antivirals during an influenza pandemic, *BMC Infectious Diseases* 9 (2009) 117.
- [15] V. Davey, R. Glass, H. Min, W. Beyeler, L. Glass, Effective, robust design of community mitigation for pandemic influenza: a systematic examination of proposed US guidance, *PLoS ONE* 3 (7) (2008) e2606.
- [16] V. Lee, D. Lye, A. Wilder-Smith, Combination strategies for pandemic influenza response - a systematic review of mathematical modeling studies, *BMC Medicine* 7 (2009) 76.
- [17] United Nations, World Population Prospects - The 2006 Revision (2007).
- [18] European Commission, Key Data on Education in Europe 2005 (2005).
- [19] S. Merler, M. Ajelli, The role of population heterogeneity and human mobility in the spread of pandemic influenza, *Proceedings of the Royal Society B* 277 (2010) 557–565.
- [20] M. Gonzalez, C. Hidalgo, A.-L. Barabasi, Understanding individual human mobility patterns, *Nature* 453 (5) (2008) 779–782.
- [21] H. Matsumoto, International urban systems and air passenger and cargo flows: some calculations, *J Air Transp Manag* 10 (4) (2004) 239–247.
- [22] T. Grosche, F. Rothlauf, A. Heinzla, Gravity models for airline passenger volume estimation, *J Air Transp Manag* 13 (4) (2007) 175–183.
- [23] C. Viboud, O. N. Bjornstad, D. L. Smith, L. Simonsen, M. A. Miller, B. T. Grenfell, Synchrony, waves, and spatial hierarchies in the spread of influenza, *Science* 312 (5772) (2006) 447–451.
- [24] D. Brockmann, L. Hufnagel, T. Geisel, The scaling laws of human travel, *Nature* 439 (2006) 462–465.
- [25] D. Balcan, V. Colizza, B. Goncalves, H. Hud, J. Ramasco, A. Vespignani, Multiscale mobility networks and the spatial spreading of infectious diseases, *Proc Natl Acad Sci USA* 106 (51) (2009) 21484–21489.
- [26] R. M. Anderson, R. M. May, *Infectious diseases of humans: dynamics and control*, Oxford, UK: Oxford University Press, 1992.
- [27] European Centre for Disease Prevention and Control, Annual Epidemiological Report on Communicable Diseases in Europe 2008 (2008).
- [28] V. Colizza, A. Barrat, M. Barthélemy, A.-J. Valleron, A. Vespignani, Modeling the worldwide spread of pandemic influenza: baseline case and containment interventions, *PLoS Med* 4 (1) (2007) e13.
- [29] J. Mossong, N. Hens, M. Jit, P. Beutels, K. Auranen, R. Mikolajczyk, M. Massari, Social Contacts and Mixing Patterns Relevant to the Spread of Infectious Diseases, *PLoS Med* 5 (3) (2008) e74.
- [30] E. Zagheni, F. Billari, P. Manfredi, A. Melegaro, J. Mossong, W. Edmunds, Using Time-Use Data to Parameterize Models for the Spread of Close-Contact Infectious Diseases, *Am J Epidemiol* 168 (9) (2008) 1082–1090.
- [31] P. Poletti, B. Caprile, M. Ajelli, A. Pugliese, S. Merler, Spontaneous behavioural changes in response to epidemics, *J Theor Biol* 260 (1) (2009) 31–40.